eJSE International

Electronic Journal of Structural Engineering 13(1) 2013

The Use of Fibre Bragg Grating To Monitor the Early Age Curing Temperature of Cement Paste

L. DONG, Z. IBRAHIM, Z. ISMAIL

Department of Civil Engineering, University of Malaya, Kuala Lumpur, Malaysia

Email: wmluodong1234@yahoo.com.cn

ABSTRACT:

In this paper, a Fibre Bragg Grating (FBG) is used to monitor the early age curing temperature of cement paste. The FBG is inscribed by a Continuous Wave (CW) 244nm argon ion laser in the photosensitive fibre. The fabricated FBG is calibrated from room temperature to 105ºC. In this temperature range, the FBG is found to be in good conditions in both the sensitivity and linearity, which are around 9pm/ºC and 99.9%, respectively. In the experiment, the GP Portland cement, sand and water were mixed by volume of 800, 500, and 275 ml, respectively, as the host specimen. The results of the experiment prove that the FBG can determine the setting time of the specimen at the curing time of 5h.

1 INTRODUCTION

Early-age cracking can be a significant problem in concrete. Cracks can develop when the tensile stress due to the volume changes in concrete exceeds the tensile strength, which is generally only 10% of the compressive strength (Lothenbach et al., 2005). At early ages, this strength is still developing while stresses are generated by volume changes. The volume of concrete begins to change shortly after it is cast and the early volume changes within 24 hours can influence the tensile stress and crack formation in hardened concrete. The early-age volume change is related to the chemical shrinkage, autogenous shrinkage, creep, swelling, and thermal expansion (Escalante-Garcia and Sharp, 2001). The increasing curing temperature can promote the hydration process leading to high early strength. As cement hydrates, the reaction provides a significant amount of heat. In large elements, this heat is trapped and can induce significant expansion. When thermal changes are superimposed upon autogenous shrinkage at early age, cracking can occur. In particular, differential thermal stress can occur due to the rapid cooling of massive concrete elements (Price, 1951; Escalante-Garcia and Sharp, 1998; Komonen and Penttala, 2003). As such, the temperature monitoring and control are most important during the casting of concrete structures.

Conventionally, the temperature monitoring for concrete structures can be carried out by the use of a thermocouple embedded in the cement paste (Bushnell-Watson and Sharp, 1986; Bushnell-Watson and Sharp, 1990a; Bushnell-Watson and Sharp, 1990b). Generally, although the thermocouple can provide temperature measurement with an acceptable accuracy, it is a typical point sensor that only provides the temperature measurement of a certain position. In recent decades, optical fibre sensors have been utilized in the composite materials field because of their numerous advantages, such as small size, low cost, and capability of avoiding electromagnetic influence (Glisic and Simon, 2000). In the late 1980s, the Fibre Bragg Grating (FBG) sensor, one kind of optical fibre sensor, attracted considerable attention to applications in the spheres of aerospace, structural, medical and chemical (Slowik et al., 2004; Allan et al., 2007; Okabe et al., 2002). Subsequently, the FBG received more research attention in optical communication and sensing applications, especially in the sensing of temperature and strain.

Thus, in this paper, the early age curing temperature of cement paste is monitored by using the FBG as the temperature-sensing element. The FBG temperatures sensing principle, FBG fabrication, temperature-wavelength calibration, experiment preparation are described in detail in this paper. The results of the experiment prove that the FBG is a good candidate in the sensing of the early-age curing temperature of cement paste.

2 FBG TEMPERATURE SENSING PRINCIPLE

The basic principle of operation of an FBG-based sensor system lies in the monitoring of the shift in wavelength of the returned "Bragg" signal, as a function of the measure (e.g., strain, temperature). The Bragg wavelength, λ_B, is related to the effective refractive index of the material, n, and the grating pitch, Λ,

$$\lambda_B = 2n\Lambda \tag{1}$$

A narrow spectral component centred on the Bragg wavelength λ_B is reflected by a FBG, when the light from a broadband light source is injected into the fibre. In the application of temperature sensing, the thermal response of FBG rises due to the inherent thermal expansion of the fibre material and the temperature dependence of the refractive index. Thus, the shift in resonance wavelength λ_B with temperature can be expressed as,

$$\Delta\lambda_B = 2n\Lambda(\alpha + (dn/dT)\Delta T/n) \tag{2}$$

where α is the thermal expansion coefficient of the fibre material, ΔT is the temperature change, dn/dT is the thermal optic coefficient of the fibre material.

From Eq.(2), the resonance wavelength is modulated by the changing of temperature, and the temperature measurement can be obtained by

$$T_m = T + \Delta\lambda_B \tag{3}$$

where T_m is the temperature measurement, T is the initial start temperature, S is the temperature-wavelength sensitivity of FBG; it needs calibrating before FBG is used. However, care must be paid to the cross-sensing of FBG in the temperature and strain due to the sensing principle of FBG, which monitors the change of grating period. Thus, the experiment should be designed carefully to avoid the strain effect.

3 FBG FABRICATION

A configuration of the FBG fabrication set up is shown in Figure 1. In this setup, an Amplified Spontaneous Emission (ASE) is used as the broadband light source. A 244nm light beam is emitted from an argon ion laser and then reflected by a mirror and expanded with two circular lenses. The light is then focused by a cylindrical lens and passed through a phase mask (with pitch 1026.8nm) before being exposed to UV light on a bared photosensitivity fibre (fibre which has been stripped off its' protective polymer coating, because the UV light cannot pass this type of protection layer). After the light passed through the phase mask, three interfering beams are generated close to the fibre, as shown in Figure 2. In this figure, the good condition of the phase mask should generate the zero order beam power as low as possible in order to achieve higher interference beam power in both +1 order and -1 order. The phase mask is placed just alongside the fibre with its mask pattern perpendicular to the fibre and the laser. The fibre is placed in near contact with the fine corrugations of the phase mask before writing. Care must be taken in the alignment process to ensure the fibre cannot come into contact with the phase mask otherwise the phase mask might be damaged. In our experiment, the FBGs are inscribed in single mode high-germania boron co-doped fibres. One of the fabricated FBG is shown in Figure 4 (a). The FBG spectrums monitor both reflection and transmission in-situ by using an Optical Spectrum Analyser (OSA).

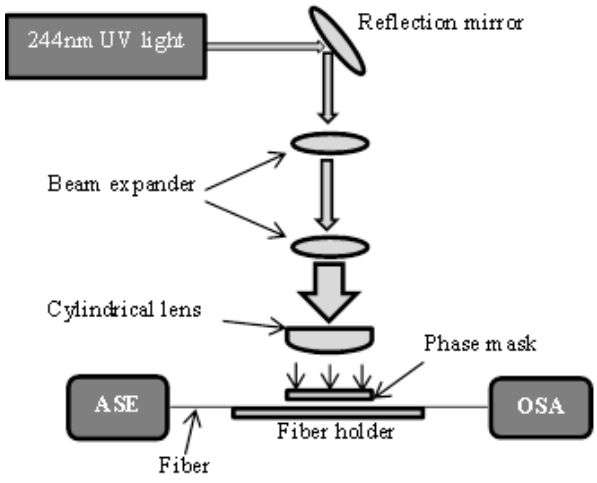

Figure 1: FBG fabrication set up using phase mask approach.

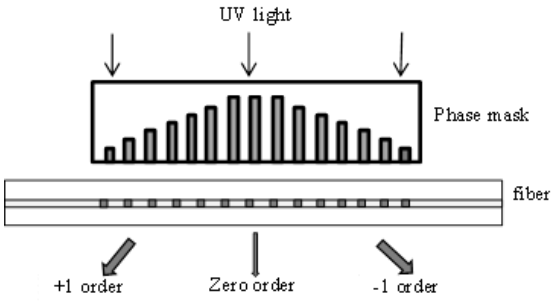

Figure 2: The interfering beams generated by phase mask.

3.1 Sensor temperature-wavelength calibration

Before embedding the FBG into the cement paste it is better to calibrate the wavelength shift with the change of temperature. A furnace with a temperature resolution ±0.5ºC is used and the climbing temperature step is set to 1ºC/mins. The wavelength shift data is recorded by the temperature increase and decrease at every 10ºC. When the temperature is reached at each increase/decrease of 10ºC points, the furnace will be held at these points for around 5 mins to stabilize the temperature and FBG response. The FBG temperature-wavelength calibration result is shown in Figure.3. From this figure, it can be observed that both the calibration curves are shown in good linearity and sensitivity and agree with each other. A sensitivity of 9pm/ºC is found for both the increase/decrease temperatures. From the sensitivity data, a temperature response of the gratings can be obtained by capturing the wavelength shift information when the FBG is used in a thermal environment.

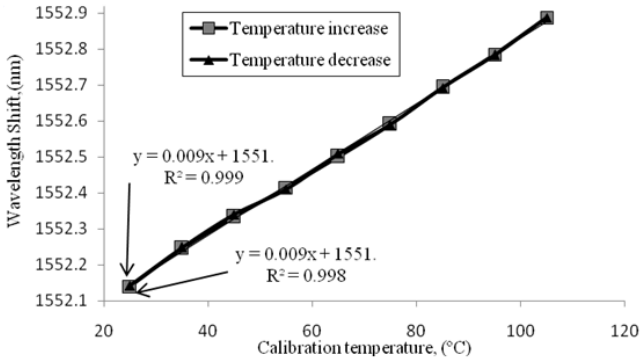

Figure 3: FBG temperature-wavelength calibration figure.

4 EXPERIMENTAL WORKS

4.1 Experimental procedure and setup

Prior to pouring the cement paste into the mould the fibre is fastened on a steel wire to avoid the effect of micro-bending and the sensing tip is inserted into a glass tube to protect it from the effect of the strain. The glass tube has an inner and outer diameter of 200um and 250um, respectively. The glass tube is also fastened by the steel wire. The steel wire is inserted parallel through the centre of the mould, as shown in Figure 4 (b). The size of the mould is 75×75×200 mm and a plastic sheet is used to cover the mould to prevent water evaporation after the pouring of the cement. The cement used is GP Portland cement compliant with AS3972. The specimen of cement paste (Figure 4(c)) has the mix proportion by volume of 800 ml, 500ml, and 275 ml for the cement, sand and water, respectively. They were mixed in a container for 2 minutes and poured into the mould slowly to prevent bending of the steel wire. The mould was vibrated for 15 seconds by hand and the data recording/monitoring system was started immediately (Dong et al., 2011). During the experiment, the room temperature was kept at 25 °C. The experiment setup is shown in Figure 4 (c). In this figure, the broadband light is emitted from an ASE source, passed through an optical circulator and then reaches the FBG sensing element. Part of the light is reflected by the grating to form a resonance peak. This resonance peak is fed back and channelled by the optical circulator again, and detected and recorded by an OSA.

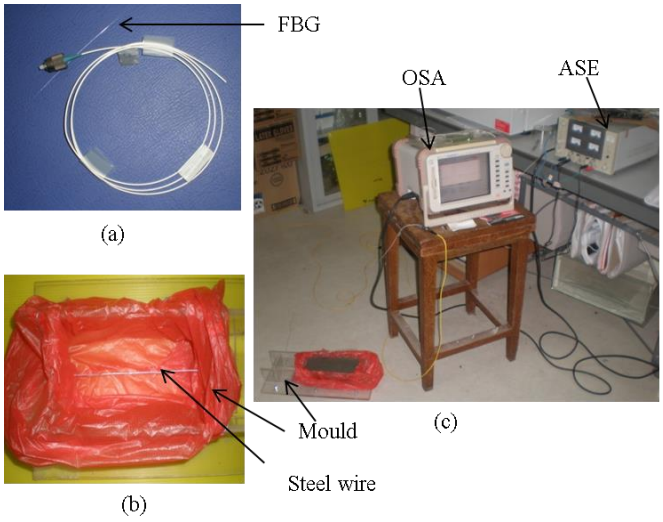

Figure 4: Experiment preparation and setup of FBG monitoring approach.

4.2 Experiment results

The measurement of the early-age curing temperature of the cement paste at the first 19 h after casting is shown in Figure 5. This figure is plotted based on Eq. (3), where the wavelength shift data is recorded by the OSA. In this figure, the temperature of the air is recorded before the specimen is poured into the mould. The starting point in this figure is 25ºC, which means the air is surrounded. From the figure, it can be observed that the temperature of the cement paste increases immediately after the cement paste is poured into the mould, which is due to the absorption of water during the hydration of cement. Hence, the starting point can be referred to as the initial setting time of the specimen. Furthermore, the hydration of cement is an exothermic reaction, which releases heat and results in the increase of the temperature of the specimen. The increment of the temperature is observed and reaches its peak at about 5 h. This time is treated as the final setting time of the specimen. After that, the increase in the temperature of cement paste slowed down and became almost stable after 19 h.

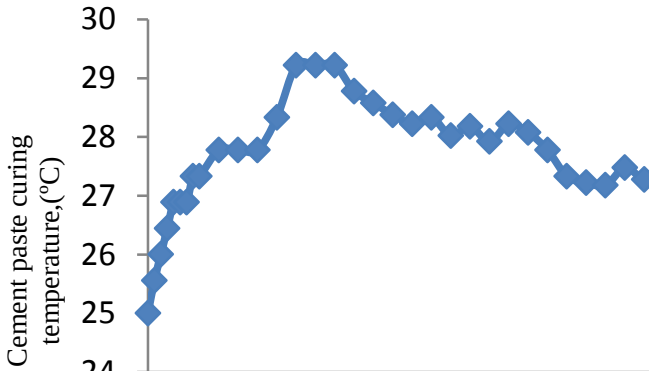

Figure 5: Measurement of the early-age curing temperature of the cement paste

5 CONCLUSION

In this paper, the FBG is used to measure the early-age curing temperature of cement paste. The FBG is fabricated by using the phase mask approach combined with a CW 244nm argon ion laser. The fabricated FBG has the sensitivity of 9pm/ºC in both increase/decrease temperatures in the temperature calibration range of 25ºC to 105ºC. In the experiment setup, a glass tube is used to protect the FBG from damage and the strain effect, where the FBG is passed through the glass tube. From the results of the experiment, we demonstrated that the FBG is a good candidate for the measurement of the early-age curing temperature of cement paste.

6 REFERENCES

Allan Wong, C. L., Childs, P. A., Berndt, R., Macken, T., Peng, G. D. and Gowripalan, N. (2007). Simultaneous measurement of shrinkage and temperature of reactive powder concrete at early-age using fiber Bragg grating sensors. Cem. Concr.Compos., 29, pp. 490-497.

Glisic, B. and Simon, N. (2000). Monitoring of concrete at very early age using stiff SOFO sensor. Cem. Concr. Compos. 22, pp. 115–119.

Lothenbach, B., Alder, C., Winnefeld, F. and Einfluss der, P. L. (2005). Temperatur und Lagerungsbedingungen auf die Festigkeitsentwicklung von Mörteln und Betonen *Beton*55 (12), pp. 604–609.

Escalante-Garcia, J.I. and Sharp, J.H. (2001). The microstructure and mechanical properties of blended cements hydrated at various temperatures. Cem. Concr. Res.31, (5), pp. 695–702.

Escalante-Garcia, J.I. and Sharp, J.H. (1998), Effect of temperature on the hydration of the main clinker phases in Portland cements: Part I, neat cements. Cem. Concr. Res.28(9), pp. 1245–1257.

Komonen, J. and Penttala, V. (2003). Effects of high temperature on the pore structure and strength of plain and polypropylene fiber reinforced cement pastes. Fire Technol.39(1), pp. 23–34.

Dong, L., Ibrahim, Z. and Ismail, Z. (2011). Monitoring of curing temperature of early age cement paste using biconical tapered fiber sensor. *Advanced Materials Research*, 250-253, 3549-3553.

Bushnell-Watson, S.M. and Sharp, J.H. (1986). The effect of temperature on the setting behavior of refractory calcium aluminate cements. Cem. Concr. Res.16, pp. 875–884.

Bushnell-Watson, S.M. and Sharp, J.H. (1990a). Further studies of the effect of temperature upon the setting behavior of refractory calcium aluminate cements. Cem. Concr. Res.20, pp. 623–635

Bushnell-Watson, S.M. and Sharp, J.H. (1990b). On the cause of the anomalous setting behavior with respect to temperature of calcium aluminate cements. Cem. Concr. Res.20 pp. 677–686.

Slowik, V., Schlattner, E. and Klink, T. (2004). Experimental investigation into early age shrinkage of cement paste by using fibre Bragg gratings. Cem. Concr. Compos. 26, pp. 473–479.

Price, W.H. (1951). Factors influencing concrete strength. J. Am. Concr. Inst.47, (31), pp. 417–432.

Okabe, Y., Yashiro, S., Tsuji, R., Mizutani, T. and Takeda, N. (2002). Effect of thermal residualstress on the reflection spectrum from fiber Bragg grating sensors embedded inCFRP laminates. Composites Part A: Applied Science and Manufacturing, 33(7), pp. 991-999.